Effects of Polymeric Electron Transporters and the Structure of Poly(*p*-phenylenevinylene) on the Performance of Light-Emitting Diodes

Marko Strukelj,*[1] Timothy M. Miller,[2] Fotis Papadimitrakopoulos,[3] and Sehwan Son

Contribution from AT&T Bell Laboratories, Murray Hill, New Jersey 07974

Received May 26, 1995[⊗]

Abstract: A series of new electroactive monomers containing 2,5-diphenyl-1,3-oxazole, 2,5-diphenyl-1,3,4-oxadiazole, and 3,4,5-triphenyl-1,2,4-triazole heterocycles have been synthesized in good yield. These monomers were incorporated as either pendant groups or directly into the backbone of 10 high molecular weight polymers [poly(arylmethacrylate), poly(arylmethacrylamide), poly(aryl formal), and poly(aryl ether)]. The polymers appear to be amorphous and exhibit glass transition temperatures in the range 115−208 °C, and most have excellent thermal stability in air (decomposition > 400 °C). Thin, clear, pinhole free-films are readily deposited on a variety of substrates (e.g., silicon, quartz) by spin coating. These materials were used as the electron transport (ET) layer in light-emitting diodes (LEDs) having an ET layer deposited on PPV with aluminum and indium tin oxide electrodes (i.e., Al/ET layer/PPV/ITO). The ET materials contain as much as 97 mol % of the electroactive moiety, while conventional electron transporters (e.g., PBD dissolved in PMMA) contain 46 mol %. LEDs containing these ET polymers were much more stable than devices without an ET. Many were also more stable than those having a conventional electron transporter. Relative to LEDs without ETs, the internal quantum efficiencies using ETs were higher in some cases and lower in others. In addition to varying the ET layer, two different types of PPV (crystalline and amorphous) were also used to construct four different types of devices. In terms of diode efficiency, the most important factor is the PPV conjugation length and not the type of ET used. The internal quantum efficiencies ranged from 0.2 to 0.0004%. Finally, the current/voltage curves of some of the LEDs were fitted to four different models in order to determine which best describes the device physics.

Introduction

Two major approaches are under study for preparing organic light-emitting diodes (LEDs). One is based on vacuum-sublimed films of low molecular weight compounds,[4] while the other uses spin-coated polymers.[5−13] Homogeneous thin films (pinhole-free down to ca. 300 Å) of low molecular weight fluorescent compounds are readily attainable by sublimation under high vacuum. However, scale-up of this deposition technique for manufacture of large displays would require considerable capital investment in order to achieve film uniformity. Furthermore, sublimed species tend to crystallize with time, and this often precipitates device failure. On the other hand, uniform thin films of polymers are readily spin- or dip-coated over large areas which would be propitious for display fabrication. Polymers can also be designed to remain amorphous, even at elevated temperatures.

Polymer-based LEDs have gained considerable attention since 1990, when Burroughes et al.[5] reported that poly(*p*-phenylenevinylene) (PPV) sandwiched in an ITO/PPV/metal device emits visible light under an applied bias. This led to the preparation of various PPV derivatives that emit light throughout the visible spectrum.[6,7,10,11]

Organic LEDs typically contain an electron transporter (ET), emitter, and hole transporter sandwiched between two electrodes. Above a threshold voltage, electrons are injected into the conduction band (LUMO level) and holes into the valence band (HOMO level) of the emitter. Recombination of holes and electrons leads to the formation of excitons, and singlet excitons which decay radiatively emit visible light. Electron and hole transporters facilitate injection of charge from the respective electrodes into the emitter. They also limit unipolar current flow and, therefore, reduce the probability of exciton formation near the electrodes and concomitant exciton quenching. Ideally, the ET layer should also induce a buildup of charges (i.e., electrons and/or holes) across the ET/emitter (e.g., PPV) interface, leading to more efficient exciton formation and

⊗ Abstract published in *Advance ACS Abstracts*, November 15, 1995.

(1) Current address: Du Pont Central Research and Development, Experimental Station, P.O. Box 80304, Wilmington, DE 19880-0304.

(2) Current address: CPS Chemical Co. Inc., P.O. Box 162, Old Bridge, NJ 08857.

(3) Current Address: University of Connecticut, Department of Chemistry/Institute of Materials Science, Storrs, CT 06269-3136.

(4) (a) For example: Tang, C. W.; VanSlyke, S. A. *Appl. Phys. Lett.* **1987**, *51* (12), 913. (b) Tang, C. W.; VanSlyke, S. A.; Chen, C. H. *Appl. Phys. Lett.* **1989**, *65* (9), 3610. (c) Adachi, C.; Tsutsui, T.; Saito, S. *Appl. Phys. Lett.* **1989**, *55* (15), 1489. (d) Adachi, C.; Tsutsui, T.; Saito, S. *Appl. Phys. Lett.* **1990**, *56* (9), 799. (e) Adachi, C.; Tsutsui, T.; Saito, S. *Appl. Phys. Lett.* **1990**, *57*, 531.

(5) Burroughes, J. H.; Bradley, D. D. C.; Brown, A. R.; Marks, R. N.; Mackay, K.; Friend, R. H.; Burn, P. L.; Holmes, A. B. *Nature* **1990**, *347*, 539.

(6) Braun, D.; Heeger, A. J. *Appl. Phys. Lett.* **1991**, *58*, 1982.

(7) Burn, P. L.; Holmes, A. B.; Kraft, A.; Bradley, D. D. C.; Brown, A. R.; Friend, R. H.; Gymer, R. W. *Nature* **1992**, *356*, 47.

(8) Brown, A. R.; Bradley, D. D. C., Burroughes, J. H.; Friend, R. H.; Greenham, N. C.; Burn, P. L.; Holmes, A. B.; Kraft, A. *Appl. Phys. Lett.* **1992**, *61* (23), 2793.

(9) Zhang, C.; Hoger, S.; Pakbaz, K.; Wudl, F.; Heeger, A. J. *J. Electron. Mater.* **1993**, *22* (4), 413.

(10) Aratani, S.; Zhang, C.; Pakbaz; Hoger, S.; Wudl, F.; Heeger, A. J. *J. Elec. Mater.* **1993**, *22* (7), 745.

(11) Greenham, N. C.; Moratti, S. C.; Bradley, D. D. C.; Friend, R. H.; Holmes, A. B. *Nature* **1993**, *365*, 628.

(12) Clery, D. Polymer Technology. *Science* **1994**, *263*, 1700.

(13) Burn, P. L.; Kraft, A.; Baigent, D. R.; Bradley, D. D. C.; Brown, A. R.; Friend, R. H.; Gymer, R. W.; Holmes, A. B.; Jackson, R. W. *J. Am. Chem. Soc.* **1993**, *115*, 10117.

0002-7863/95/1517-11976$09.00/0

improved quantum efficiency.[14] Efficient devices also require balanced injection of holes and electrons. A hole transport layer is not required for PPV-based devices because it inherently transports holes. For conjugated polymers such as PPV and its derivatives, LED efficiency has been limited by electron injection when the anode is ITO, and as a result, low work function cathode metals such as calcium have been used to provide devices with quantum efficiencies for alkoxy derivatives of up to 0.75% (photons per electron).[6,15] Unfortunately, calcium is highly reactive in air. Aluminum is a more stable electrode, but its higher work function leads to LEDs with lower efficiencies (0.002−0.1%).[16]

2-(4-Biphenylyl)-5-(4-*tert*-butylphenyl)-1,3,4-oxadiazole (PBD; see supporting information (S1)) is the most widely used ET.[14] Recently it has been shown that 3-(4-biphenylyl)-4-phenyl-5-(4-*tert*-butylphenyl)-1,2,4-triazole (TAZ) also transports electrons. It also appears to block holes more efficiently than PBD.[17] Since PBD crystallizes readily after evaporation as a thin film (ca. 500 Å), it has been dispersed in an inert amorphous polymer matrix such as poly(methyl methacrylate).[18] There are several drawbacks to embedding a small molecule ET in a polymer matrix, including (1) dilution of the electroactive component reducing the charge carrying capacity of the film;[19] (2) loading limited by solubility in the host matrix; and (3) depression of the composite glass transition temperature (T_g) due to plasticization. When PBD is embedded in PMMA by spin coating a solution of these two components, the loading is limited to ca. 46 mol %. Mild heating accelerates phase separation, resulting in poor device performance or even failure. Moreover, using PBD/PMMA as an ET in PPV-based LEDs increases operating voltages by ca. 10−15 V. This substantially decreases the power efficiency and often also reduces operational lifetimes.

We reported in a preliminary account that many of these problems can be circumvented using polymeric PBD and TAZ derivatives,[20] where the electroactive moiety is either attached as a pendant group or incorporated directly into the backbone of the polymer. The resulting poly(aryl methacrylate) and poly(aryl ether)s are soluble and amorphous and possess T_g's above 150 °C. Here we elaborate on the scope of the synthetic methodology to maximize the concentration of the electroactive moiety and to demonstrate the generality of the monomer and polymer synthetic schemes. In addition, different types of EL device architectures were prepared using two different types of PPV to determine the importance of each variable. Detailed device performance is provided describing the power efficiency and stabilities of PPV-based LEDs. Performance is shown to be strongly dependant on the ET, the composition of the PPV, and the device architecture. Finally, the current/voltage ($I-V$) profiles of some representative LEDs were fit to different models to illustrate which best describes the device physics.

Results and Discussion

Monomer Syntheses and Properties. The oxadiazole-containing biphenol **1a** (Scheme 1) is prepared in three steps from *m*-anisic hydrazide and *m*-anisoyl chloride (see supporting information (S2)). In the first step formation of a disubstituted hydrazide proceeds smoothly (81% yield) at −30 °C in DMAc. Ring closure in refluxing phosphorus oxychloride[21] gives a symmetrical oxadiazole, exclusively (87% yield), in about 1 h. Demethylation with boron tribromide in methylene chloride yields biphenol **1a** (61% yield).[22] The monophenol analogue of **1a** (see supporting information (S2)) is prepared in good yield using the same reaction sequence.

Scheme 1. Polymer Synthesis

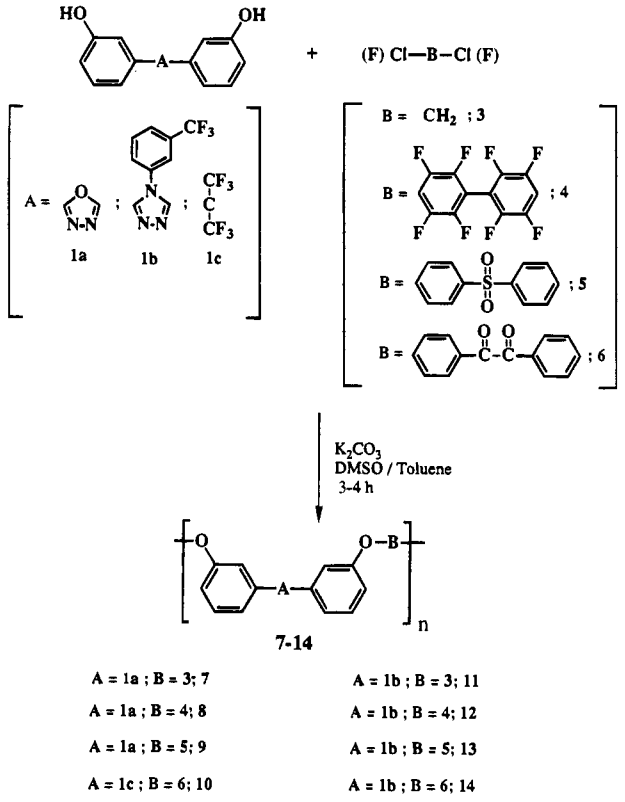

The triazole-containing biphenol **1b** (Scheme 1) is synthesized in four steps beginning with the formation of an amide by condensation of *m*-(trifluoromethyl) aniline with *m*-anisoyl chloride (84% yield) (see supporting information (S3)). The amide is then converted to the corresponding benzimidyl chloride by refluxing in thionyl chloride (65% yield). Subsequent reaction with *m*-anisic hydrazide in DMAc at 135 °C gives the substituted triazole (55% yield) which is then deprotected with boron tribromide or HBr to give biphenol **1b** (62% yield). This triazole synthesis[23] has the advantage over other approaches[24] in that triazoles containing three different aryl moieties are readily accessible. Furthermore, this route is versatile in terms of the functional groups permissible on the phenyl groups, since the nitro-substituted derivative of **1b**, 3,5-bis(*m*-nitrophenyl)-4-phenyl-1,2,4-triazole, has been prepared in similar yield using this approach.[23]

5-*p*-Aminophenyl-2-phenyloxazole is prepared in two steps (see supporting information (S4)). Nitration of 2,5-diphenyl-1,3-oxazole in fuming nitric acid at 0 °C proceeds instanta-

(14) Adachi, C.; Tsutsui, T.; Saito, S. *Appl. Phys. Lett.* **1990**, *57*, 531.
(15) Zhang, C.; Braun, D.; Heeger, A. J. *J. Appl. Phys.* **1993**, *73* (10), 5177.
(16) Bradley, D. D. C. *Synth. Met.* **1993**, *54*, 401.
(17) Kido, J.; Ohtaki, C.; Hongawa, K.; Okuyama, K.; Nagai, K. *Jpn. J. Appl. Phys.* **1993**, *32*, L917. The stability of TAZ in thin film form is not described.
(18) Brown, A. R.; Bradley, D. D. C.; Burroughes, J. H.; Friend, R. H.; Greenham, N. C.; Burn, P. L.; Holmes, A. B.; Kraft, A. *Appl. Phys. Lett.* **1992**, *61* (23), 2793.
(19) Stolka, M.; Yanus, J. F.; Pai, D. M. *J. Phys. Chem.* **1984**, *88*, 4707.
(20) Strukelj, M.; Papadimitrakopoulos, F.; Miller, T. M.; Rothberg, L. J. *Science* **1995**, *267*, 1969.
(21) Hayes, F. N.; Rogers, B. S.; Ott, D. G. *J. Am. Chem. Soc.* **1955**, *77*, 1850.
(22) This reaction is quantitative as determined by thin layer chromatography; however, the reduction in yield occurs during recrystallization. Biphenol **5a** and the para-substituted derivative have been prepared previously using a different synthetic route (Iwakura, Y.; Uno, K.; Imai, Y.; Takase, Y. *Makromol. Chemie*, **1966**, *95*, 261. Connell, J. W.; Hergenrother, P. M.; Wolf, P. *Polymer*, **1992**, *33*, 3507).
(23) Preston, J. *J. Heterocyclic Chem.* **1965**, *2*, 441.
(24) For example, Stolle, R. *J. Prakt. Chem.* **1903**, *68*, 130.

Scheme 2. Polymer Synthesis

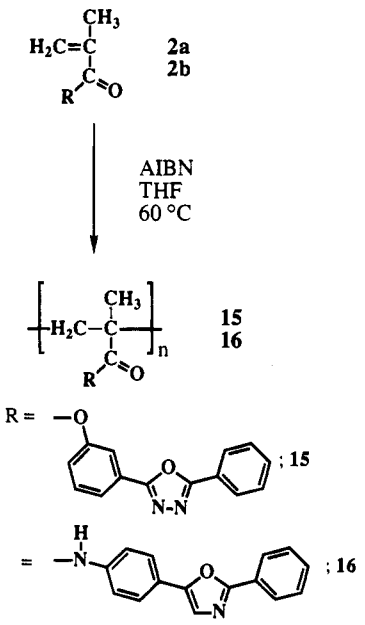

Table 1. Properties of Poly(aryl methacrylate) **15**, Poly(arylmethacrylamide) **16**, Poly(formal)s **7** and **11**, and Poly(aryl ether)s **8**–**10** and **12**–**14**

polymer	T_g (°C)	TGA (°C) (−5%)	η_{inh}[a]	GPC[b] M_w	GPC[b] M_n
15	153			27 800	12 000
16	208[c]			17 600	10 700
7[d]	115	396			
11	125	426	0.59	45 800	17 400
8	176	521	0.48	32 900	14 200
9	193	510	0.44	29 300	11 700
10	168	524	0.50	35 600	13 200
12	180	478	0.40	26 200	10 100
13	186	534	0.47	31 250	13 800
14	170	533	0.34	22 100	7 950

[a] Inherent viscosity. 0.5 g/dL in DMF at 25 °C. [b] Based on polystyrene standards in DMF. All traces are monomodal. [c] DSC scan was run at 40 °C/min in order to be able to detect a T_g. [d] Polymer could not be redissolved.

neously and gives the nitro adduct quantitatively, as described by Minovici.[25] Reduction with tin(II) chloride and HCl in glacial acetic acid gives the desired amine in good yield (80%).

The corresponding methacrylate ester **2a** and methacrylamide **2b** (Scheme 2) are prepared (83 and 85% yield) by reaction of 2-(3′-hydroxyphenyl)-5-phenyloxadiazole and 5-(*p*-aminophenyl)-2-phenyloxazole, respectively, with methacryloyl chloride in chloroform containing triethylamine.

Polymer Syntheses and Properties. Poly(aryl methacrylate) **15** and poly(arylmethacrylamide) **16** (Scheme 2) are prepared by free radical polymerization at 60 °C in THF using AIBN as the initiator. The polymers are soluble and exhibit T_g's of 153 and 208 °C (Table 1). Both polymers form clear, homogenous, and adherent thin films (ca. 500 Å) when spin-coated from dilute solution (2% w/v chlorobenzene).

The poly(formal)s **7** and **11** (Scheme 1) are prepared from the oxadiazole- and triazole-containing biphenols **1a** and **1b**, respectively, using an NMP:CH_2Cl_2 solvent mixture (3:2) at ca. 20% solids and an excess of KOH.[26] While it has been shown that polymerizations at higher solids (ca. 30% w/v) content yield fewer cyclics (e.g., 4–7%), these polymerizations had to be run at lower concentrations because the resulting polymers are considerably less soluble than those prepared by Hay et al.[26] Polymers **7** and **11** have substantially different solubilities. The oxadiazole-containing poly(formal) **7** must be prepared at ca. 135 °C because small molecule and oligomeric salts and the polymer precipitate at lower temperatures. Furthermore, after isolation, **7** is only partially soluble in chlorobenzene, cyclohexanone, or DMAc, even at low concentrations (e.g. ≤2% solids w/v). This insolubility is ascribed to the planarity of the 2,5-diphenyl-1,3,4-oxadiazole system, even though the hydroxyl groups are strategically positioned *meta* to the oxadiazole to favor solubility. The triazole-containing poly(formal) **11** is substantially more soluble, and high molecular weight polymer can be readily synthesized at 70 °C.[27] The T_g's of **7** and **11** are 115 and 125 °C, respectively, and both polymers exhibit good thermal stability in air (Table 1). While **11** can be redissolved in cyclohexanone and DMAc after isolation, once it is reprecipitated a second time to ensure that all of the salts and low molecular weight (e.g., NMP) impurities are removed, it is only soluble in DMAc at low concentrations (i.e., 2% solids w/v).

The poly(aryl ether)s **8**–**10** and **12**–**14** (Scheme 1) are prepared from the appropriate biphenol (**1a**–**c**) and activated aromatic dihalide to yield high molecular weight linear polymers using a dipolar aprotic solvent and anhydrous potassium carbonate as the base.[28] However, contrary to standard conditions which necessitate reaction temperatures of 160–170 °C and reaction times of ca. 8 h, lower temperatures (<145 °C) and shorter reaction times are employed here in order to improve the purity of the resulting polymers. Furthermore, to achieve high molecular weight polymers under these mild conditions, DMSO was substituted for NMP as the solvent. Presumably, the higher polymerization rate in DMSO is attributable to increased anion nucleophilicity due to improved cation solvation. The glass transition temperatures and thermal stabilities in air (−5% weight loss) of the polymers range from 176–193 °C and 478–534 °C, respectively (Table 1). The sulfone **13** is particularly thermally stable. Dilute solutions (2% solids w/v) of polymers **8**, **10**,[29] **12**, and **14** can be readily spin-coated to give clear and colorless thin films (ca. 500 Å). Unfortunately, the diphenyl sulfone-containing polymers **9** and **13** cannot be completely redissolved once they are purified by a second reprecipitation.

When solubilities of the triazole- and oxadiazole based polymers **8**–**10** and **12**–**14** are compared, the former are considerably higher in each case. We initially thought that this behavior might be attributable to noncoplanarity of the *meta* trifluorotolyl and triazole rings which should hinder chain packing. However, when portions of polymer chains **8** and **12** (see supporting information (S5 and S6)) were modeled (*CAChe* package[30]), to find the lowest energy structure, **12** has the

(25) Minovici, S. S. *Ber. Dtsch. Chem. Ges.* **1896**, 2097.

(26) Hay, A. S.; Williams, F. J.; Relles, H. M.; Boulette, B. M.; Donahue, P. E.; Johnson, D. S. *J. Polym. Sci., Polym. Lett. Ed.* **1983**, *21*, 449.

(27) A chain stopper (1–2%) was used to prevent the molecular weight from becoming too high.

(28) (a) For example: Johnson, R. N.; Farnham, A. G.; Clendinning, R. A.; Hale, W. F.; Merriam, C. N. *J. Polym. Sci.* **1967**, A-1, *5*, 2375. (b) Heath, D. R.; Wirth, J. G. U.S. Patent 3,730,946, 1973 (General Electric). (c) Feasey, R. G. U.S. Patent 3,918,587, 1974 (Imperial Chemical Industries). (d) Taylor, I. C. U.S. Patent 4.105,636, 1978 (Imperial Chemical Industries). (e) Takekoshi, T.; Wirth, J. G.; Heath, D. R.; Kochanowski, J. E.; Manello, J. S.; Weber, M. J. *J. Polym. Sci., Polym. Chem. Ed.* **1980**, *18*, 3069. (f) White, D. M.; Takekosi, T.; Williams, F. J.; Relles, H. M.; Donahue, P. E.; Klopfer, H. J.; Loucks, G. R.; Manello, J. S.; Mathews, R. O.; Schluenz, R. W. *J. Polym. Sci., Polym. Chem. Ed.* **1981**, *19*, 1635.

(29) Strukelj, M.; Hedrick, J. C.; Hedrick, J. L.; Twieg, R. J. *Macromolecules* **1994**, *27*, 6277.

(30) The Computer Aided Chemistry molecular modeling program (CacheTM, Version 3.0; CAChe Scientific, 18700 N.W. Walker Rd., Bldg. 92-01, Beaverton, OR 97006) implements Allinger's standard MM2 force field to find the optimum molecular geometries (Allinger, N. L.; et al. *J. Am. Chem. Soc.* **1977**, *99*, 8127).

Table 2. Electroluminescent Behavior of Devices Depicted in Figure 1

device	electron transporter (ET)	internal quantum efficiency (%)	stability[a] (C/cm2)
type 1 (double-layer PPV)	PBD/PMMA	0.004−0.002	~1
	15, **16**, **11**, **8**, **10**, and **12**	0.004−0.002	5−≫20
type 2 (single-layer PPV)	PBD/PMMA, **15**, **16**, **11**, **8**, **10**, and **12**	0.03−07	≪1
type 3 (methoxy-modified PPV)	PBD/PMMA	0.15−0.25	≪1
type 4 (PPV derived from xanthate precursor)	No ET	0.05−0.1	NA[b]
	PBD/PMMA	0.22 (ref 31)	NA[b]
	15	0.1−0.2	NA[b]
	PBD/**15**	0.2−0.6	NA[b]
	12 and **14**	0.03	NA[b]

[a] Stability was measured by pulsating the current from 0−250 uA. The stability value reported is the amount of charge passed through the LED before failure, and the number of photons emitted is 1.2×10^{14} times this value. [b] Not available at this time.

trifluorotolyl and triazole rings essentially coplanar (0.5°) while the chain aryl rings are nearly orthogonal (85°) to the triazole. In fact, the structural energy of **12** with the trifluorotolyl and triazole rings orthogonal is 55 kcal/mol higher, and subsequent energy minimization from such a conformer results in reversion back to the coplanar structure. The lowest energy structure for the oxadiazole-containing chain segment indicates the phenyl moieties are essentially coplanar (5°) with the oxadiazole ring. This conformation presumably explains the poorer solubilities of polymers prepared from biphenol **1a**.

Morphological Behavior of PBD Dissolved in PMMA. In order to try to understand the poor storage stability of LEDs having PBD/PMMA as an ET (*vide infra*) and the phase behavior of these solid solutions, we examined their thermal and optical properties by differential scanning calorimetry (DSC) and optical microscopy. Both approaches show that PBD in a solid solution of 3:1 (wt/wt) PBD:PMMA forms spherulites on heating to 59 °C. The PBD:PMMA sample used in the DSC analysis (ca. 10 mg) was prepared in the melt yielding a clear and almost colorless solid upon cooling. Attempts to prepare homogeneous films (e.g., ca. 50 μm thick) by solution casting with slow solvent evaporation yielded only opaque, phase-separated films. The DSC thermogram of a PBD:PMMA sample exhibited an exothermic peak at 59−61 °C and an endothermic peak at 132−136 °C (see supporting information (S7)). After rapid cooling from 140−30 °C, the sample's appearance was unchanged. The endotherm at 132−136 °C corresponds exactly to the melting of pure PBD (see supporting information (S7)). In order to monitor the morphological changes induced by heating, a sample was observed under an optical microscope equipped with cross-polarizers. At 25 °C, the sample appears nonbirefringent (see supporting information (S8)). Upon heating, small crystals form throughout the sample at temperatures above 59 °C, resulting in an opaque phase-separated sample. At temperatures above 132 °C, the PBD melts and redissolves in PMMA ($T_g \cong 105$ °C) to form a clear homogeneous mixture again. Subsequent *slow* cooling (10 °C/min) from 140−30 °C results in the formation of large spherulites (see supporting information (S9)) at 79 °C. The propensity of PBD to crystallize is also visible in actual bilayer LEDs using this electron transport system (Al/PBD in PMMA/PPV/ITO). Similar crystallites are clearly detectable after 1 month of storage (see supporting information (S10)). The size and shape of these crystals closely resemble those formed when a PBD/PMMA sample was heated. We conclude that these 3:1 solutions of PBD in PMMA are thermodynamically unstable relative to a two-phase system containing crystalline PBD.

LED Fabrication and Strategy. In general, our LEDs consisted of two thin organic layers sandwiched between aluminum and indium tin oxide (ITO) electrodes (Figure 1).

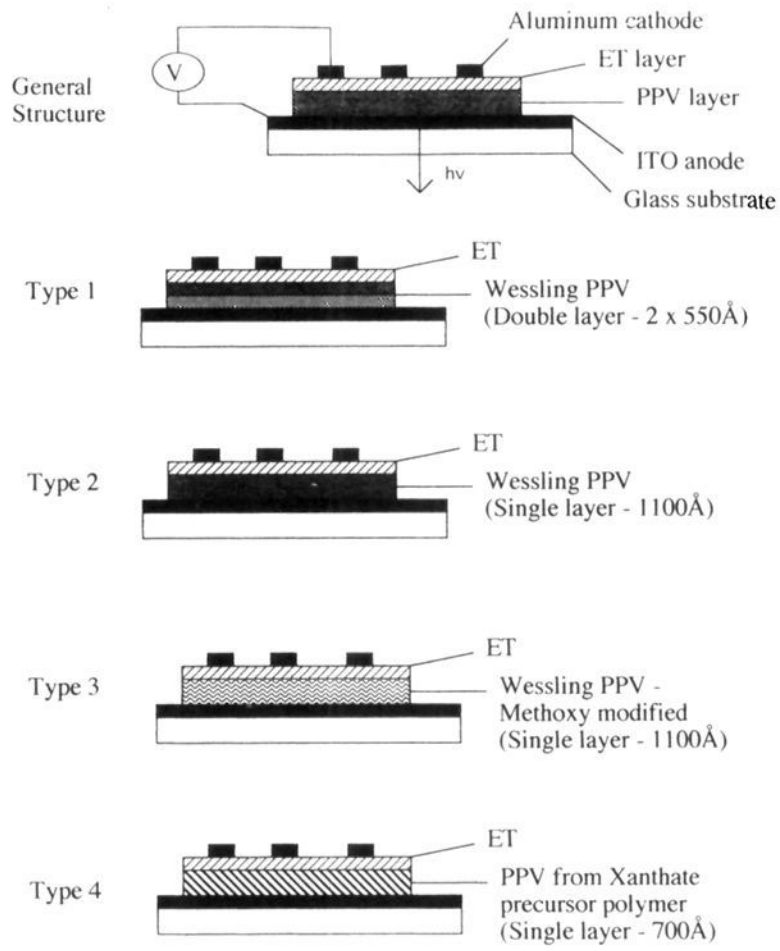

Figure 1. LED device schematic.

The first layer is the emitter-hole transporter, PPV, and the second is a polymeric ET. Both layers are deposited by spin coating. The PPV is prepared from either the tetrahydrothiophenium chloride salt Wessling precursor polymer or the organic soluble xanthate precursor polymer recently described by Son et al.[31] The former is converted at 200 °C under an atmosphere of 15% H_2 in N_2, while the latter is converted at 180 °C under Ar. LEDs containing a PBD:PMMA ET and no ET (i.e., only PPV) were also prepared to permit direct side by side comparisons to be made between the polymeric ETs (**15**, **16**, **7**, **8**, **10**, **12**, and **14**) and previously reported systems. While the ET is always deposited as a single layer (450−500 Å), PPV obtained from the Wessling route is deposited either as a *single* layer (1100 Å) or as a *double* layer (2 × 550 Å; *vide infra*). The xanthate precursor polymer is always applied as a *single* layer (700 Å).

In all, four types of LEDs were prepared in order to study the importance of film uniformity and interface differences (i.e., ET/Wessling PPV and ET/xanthate PPV) in determining diode efficiency, stability, and yield (Figure 1). The behavior of the devices is described below, and the results are summarized in Table 2.

Diode Stability and Yield. The LEDs are 1 mm^2 in area and are driven with direct currents up to 5 A/cm^2, which requires biases of 10−60 V. For LEDs containing PPV prepared by the Wessling route, the most important factors in determining

(31) Son, S.; Galvin, M.; Lovinger. *Science* **1995**, *269*, 376.

diode stability[32] and yield are the type of electron transporter, the number of layers of PPV [i.e., single layer vs double layer; Figure 1 (types 1 and 2)], and PPV conjugation length (type 3).

All devices having a *double* layer [2 × 550 Å; Figure 1 (type 1)] of PPV and the ETs **15**, **16**, **11**, **8**, **10**, **12**, and **14** exhibited consistently smooth and reproducible $I-V$ behavior with virtually no change in curve shape after being driven several hundred times from 0 to 25 mA/cm^2, which corresponds to a total charge passed of 15 C/cm^2. LEDs containing PBD/PMMA as the ET are stable up to currents of only 10 mA/cm^2, and usually fail by shorting after 10−20 applications of 25 mA/cm^2. When higher currents are employed (i.e., ≫25 mA/cm^2) LEDs containing **15** and **16**, and **12** are the least and most stable, respectively. For example, when the current is ramped in 100−200 μA increments, diodes prepared using polymer **12** permitted passage of currents as large as 3 ± 0.5 A/cm^2 before failure, whereas those using **15** and **16** fail when driven with 200 ± 30 mA/cm^2. When PBD/PMMA is the ET, devices fail when only 100 ± 20 mA/cm^2 is exceeded. This behavior might correlate with turn-on voltages which are the highest for **15** and **16** and the lowest for **12.** The surprisingly high current carrying capacity of LEDs containing **12** must be related to its chemical composition, since **15**, **16**, **11**, **8**, **10**, **12**, and **14** are all amorphous and have similar T_g's. LEDs without an ET are much less stable than the poorest PBD/PMMA ET containing devices.

Diodes containing a *single* layer [1100 Å; Figure 1 (Types 2 and 3)] of PPV and an ET exhibit highly erratic $I-V$ characteristics and fail after only 5−10 scans from 0 to10 mA/cm^2, and it is difficult to distinguish diode performance as a function of the ET for PPV prepared by the Wessling route. In general, for devices with an ET, the yield of functional LEDs having a *double* layer of PPV (type 1) is >95%, but the yield of LEDs having a *single* layer of PPV (type 2) is only ca. 10%. We attribute this behavior to fewer overlapping pinholes in the two PPV layers. Pinholes and other microscopic defects presumably become prominent in PPV prepared by the Wessling procedure due to film shrinkage, caused by crystallization,[33] during conversion from the precursor into PPV. This explanation appears to be corroborated by the recent results of Son et al.,[31] who obtained a high yield of LEDs from thin single-layer films [700 Å; Figure 1 (type 4)] using a new type of PPV, that is amorphous, as revealed by electron diffraction, and presumably forms more homogeneous films because of less shrinkage during the conversion step. The amorphous morphology is attributed to the presence of some *cis* double bonds along the polymer backbone which interfere with chain packing.

LEDs prepared using PBD/PMMA degrade rapidly on storage in an Ar-filled drybox at room temperature. The films became cloudy, and the devices are less stable within days of preparation. We attribute this behavior to crystallization of the PBD (*vide supra*; see supporting information (S10)). LEDs prepared from polymeric ETs **15**, **16**, **11**, **8**, **10**, **12**, and **14** show no change in performance even after several months of storage, and the films remain clear and homogeneous. The difference in behavior of these two types of ETs illustrates the importance of using materials with high T_g's and covalently attached electroactive components to suppress phase separation and improve device longevity.

Diode Operating Voltage. The operating voltages for these devices must be low enough to be compatible with display drive electronics. The low turn-on voltages (6−10 V) of devices using polymer **12** are remarkable, since this is 8−20 V lower than those of the other devices and is in the range for PPV (ca. 6 V) devices without an electron transport layer. The exceptional behavior suggests that electron mobility in **12** or injection of electrons from **12** into PPV is significantly more facile than for the other ET materials.

Diode Efficiency. For PPV prepared according to the Wessling route, the internal quantum efficiency varies *inversely* with stability. *Single*-layer PPV (Figure 1; type 2) based devices using PBD/PMMA exhibit efficiencies in the range 0.03−0.07% (Table 2). *Double*-layer PPV (Figure 1; type 1) devices using PBD/PMMA, **15**, **16**, **11**, **8**, **10**, and **12** as the ET are substantially lower, 0.0004−0.002%. Interestingly, the efficiencies in the latter are almost the same for all of the devices, even though different ET materials were used. When the conjugation length of the single-layer PPV (Figure 1; type 3) is reduced by displacement of the tetrahydrosulfonium group with methanol, according to published procedure,[34] the efficiencies for devices employing PBD/PMMA as the ET layer increase even further (~0.2%) as has been reported. However, a concomitant dramatic decrease in diode stability is also observed. The efficiency decreases by a factor of 10, after only 10−20 scans in air. Clearly, subtle differences in the PPV chemical composition and morphology of the PPV or the PPV/PPV interface (*double*-layer devices) exert the most profound effect on diode efficiency, while the role of the ET layer is to stabilize the diode.

Even though it is difficult to make direct comparisons of efficiencies in devices using PPV that is prepared by the Wessling route, due to the poor stability of devices without an ET and the low quantum efficiencies with an ET, LEDs using PPV prepared by the nonionic xanthate precursor route allow direct comparisons of efficiencies in devices with and without ET layers to be made. Internal quantum efficiencies in LEDs without an ET are in the range 0.05−0.1%, which are significantly greater than efficiencies we obtain for devices having PPV prepared by the Wessling route (i.e., up to 0.002% for double-layer PPV),[20] and are similar to the results recently described by Son et al.[31] With more efficient LEDs it also seemed likely that we could observe a dependence of efficiencies on the ET, and we did. LEDs containing ET polymers **12** and **14** have internal quantum efficiencies of ca. 0.03%. We do not understand why they decrease. LEDs containing **15** have efficiencies of ca. 0.1−0.2%, which are approximately twice the efficiencies of LEDs without an ET layer. Device efficiency is further improved by using a solution of PBD in **15**, instead of PMMA. The efficiency of an LED having a 3:1 PBD:**15** mixture is 0.2−0.6%, comparable to that obtained from devices containing PBD in PMMA layers.

Band Offsets of LUMO Energy Levels. Recently, several groups have reported that the $I-V$ characteristics and efficiencies of polymeric LEDs, with or without an ET layer, can be explained by the energy differences between the conduction and valence levels in the semiconducting organics and the work functions of the electrodes or the so-called band offsets.[11,35,36] It has been proposed that lowering the LUMO or conduction level energy of the ET gives a closer match to the work function of aluminum and that this results in enhanced efficiencies by facilitating injection of electrons into the emitting layer.[11,35,36]

(32) We tested our LEDs in the dark in air which means our stability data should be regarded as a lower bounds on the intrinsic operational stabilities.

(33) Garnier et al. have observed sharp and discrete crystallographic reflections in PPV prepared according to the procedure of Wessling (*J. Polym. Sci., Part B: Polym. Phys.* **1986**, *24*, 2783).

(34) Burn, P. L.; Holmes, A. B.; Kraft, A.; Bradley, D. D. C.; Brown, A. R.; Friend, R. H. *J. Chem. Soc., Chem. Commun.* **1992**, 32.

(35) Parker, I. D.; Pei, Q.; Marrocco, M. *Appl. Phys. Lett.* **1994**, *65* (10), 1272.

(36) Parker, I. D. *J. Appl. Phys.* **1994**, *75*, 1656.

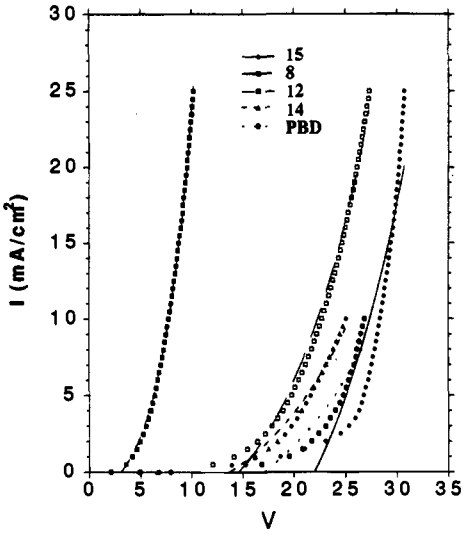

Figure 2. Current/voltage plots for the LEDs having 1100 Å of PPV (double-layer) prepared by the Wessling route, ca. 450 Å of an ET layer, and ITO and aluminum electrodes. The symbols are data points, and the lines are fits to the diode equation $I \propto \exp(aV) + b$.

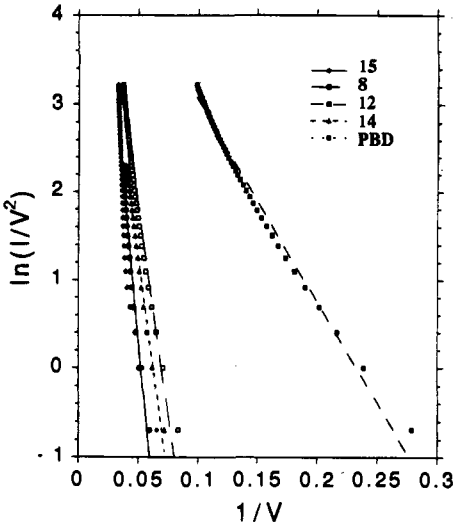

Figure 3. Fowler–Nordheim plot for LEDs described in Figure 2. The symbols are data points, and the lines are fits to the equation $\ln(I/V^2)$ vs $1/V$.

We recently showed that there was no correlation between the reduction potentials of the components of the ET materials and the operating voltages or efficiencies of the corresponding LEDs.[20] This result has several implications for the mechanism of electroluminescence in these devices. First, it indicates that the $I-V$ characteristics are only partially governed by band offsets. Second, because there are significant differences in the turn-on voltages of our LEDs, but no difference in quantum efficiencies, either the hole mobility in PPV is governing the $I-V$ properties or, more likely in our opinion, the mechanism of operation changes as a function of the ET material (*vide infra*). We assume that the invariance of the quantum efficiencies with ET polymer implies that the probabilities of making emissive excitons are the same.[37] If this is true it may imply that the mechanism shifts from one limited by mainly charge injection for LEDs having the high turn-on voltages to one limited more by space–charge effects for LEDs having **12** as the ET polymer. This assumption is supported by curve fitting our $I-V$ data to various models for this series of LEDs.

Fitting the ET/PPV $I-V$ Curves to Models. We fitted the $I-V$ curves of our LEDs (Figure 1; type 1) having PBD/PMMA, **15**, **8**, **12**, and **14** as ET layers on PPV prepared by the Wessling route to four different models to determine which best describes the device behavior under applied field. The first model was a power law in which $I \propto V^x$. This model has been used by Forrest et al. to explain the $I-V$ characteristics of ITO/diamine/Alq_3/Mg–Ag LEDs, and in it, current is governed by trap-limited transport of one of the charge carriers.[38] Of the four models the $I-V$ plots give the poorest fit to the power law. A second model which might be expected to fit the data is the diode equation in which $I \propto \exp(aV) + b$.[38] The $I-V$ curve for the LED with **12** fit this model well but the other LEDs do not (Figure 2). A good data fit to this expression is usually interpreted to mean that thermionic emission across a junction is limiting the current. We obtained good fits of our data to the Fowler–Nordheim injection model used by Parker to explain the $I-V$ characteristics of a series of LEDs having MEH-PPV as the emitter and electrodes of widely varying work functions.[36] However, **12** can be fit better to the diode equation. Plots of $\ln(I/V^2)$ versus $1/V$ yield straight lines especially above the turn-on voltages of these devices (Figure 3). This behavior indicates that current is controlled by a tunneling process which we assume is electrons across the aluminum/ET barrier or the ET/PPV barrier. The slopes of the lines in Figure 3 should be related to a barrier height, and the smaller slope for LEDs with **12** indicates that it has a lower barrier which is qualitatively consistent with its lower turn-on voltage. The last model we tried to fit the data to was the space–charge limited expression used by Stolka et al. to explain the charge transport properties of solutions of low molecular weight compounds in inert polymers.[19] Here $I \propto aV^2$, and for this model, good agreement is found only for LEDs having **12** as the ET (see supporting information (S11)). We believe that the good fit of the $I-V$ curve of the LED having **12** as the ET to both a diode and a space-charge limited current model, while other LEDs cannot be fit, indicates that a shift in mechanism takes place for these LEDs. The mechanism changes from one in which electron current is limited by injection (i.e., Fowler–Nordheim) to one in which either transport or thermionic emission of electrons dominates the $I-V$ characteristics.

(37) Yan, M.; Rothberg, L. J.; Papadimitrakopoulos, F.; Galvin, M.; Miller, T. *Phys. Rev. Lett.* **1994**, *72*, 104.
(38) Burrows, P. E.; Forrest, S. R. *Appl. Phys. Lett.* **1994**, *64* (17), 2285.

Summary

A series of novel substituted oxadiazole-, oxazole-, and triazole-containing electroactive active monomers have been synthesized and subsequently incorporated into high molecular weight polymers where the electroactive unit is either pendant to the polymer chain or part of the backbone. In all cases the electroactive unit is present in each repeat unit. The polymers were prepared by free radical polymerization or by condensation polymerization in a dipolar aprotic solvent in the presence of base. All of the polymers are amorphous, and most are soluble in solvents such as chlorobenzene, cyclohexanone, or dimethylacetamide, allowing simple deposition by spin coating to give high-quality films. The T_g's range from 115 to 208 °C, and these materials exhibit good thermal and morphological stability in air at elevated temperatures. The conventional electron transport material PBD dissolved in a PMMA matrix was shown to be thermodynamically unstable, due to phase separation induced crystallization of PBD.

The internal quantum efficiencies using polymeric ETs are higher in some cases and lower in others, relative to LEDs without ETs. The behavior depends on which ET is combined with which type of PPV (i.e., Wessling vs xanthate). Furthermore, for LEDs having PPV prepared according to Wessling,

efficiencies do not change with ET. In general, however, the PPV conjugation length appears to exert the most profound effect on diode efficiencies, which ranged from 0.0004 to 0.2%. The most efficient devices are the least stable. LEDs containing these ET polymers were dramatically more stable than devices without an ET layer. Most were also more stable than LEDs having a PBD/PMMA electron transporter. The operational stabilities and maximum current prior to device failure of LEDs prepared with several of these polymeric transporters are enhanced by factors of >20 and 30, respectively, over those having PBD in PMMA as the electron transport material. Diodes having polymer **12** as the ET material had turn-on voltages essentially indistinguishable from LEDs without an ET layer. When $I-V$ curves for some representative LEDs are fitted to different models to determine which best describes the device physics, there is evidence for a change in mechanism for ET **12**. One limitation of these materials, as with any polymer, is that the solubility of the underlying layer must be sufficiently low to prevent dissolution during deposition. However, it has been reported that a PBD/PMMA mixture can be deposited onto a soluble polymer, even though the experimental method was not described.[35,39] The principles, conclusions, and materials described here are likely to find use in LEDs having other p-type emitters or in other types of devices in which an n-type semiconductor is desired.

Experimental Section

Materials. *m*-Anisoyl chloride, *m*-Anisic hydrazide, 3-aminobenzotrifluoride, 2,5-diphenyl-1,3-oxazole, decafluorobiphenyl, 4,4′-difluorobenzil, 4,4′-difluorodiphenyl sulfone, anhydrous potassium carbonate, tin(II) chloride, benzoyl chloride, thionyl chloride, phosphorus oxychloride, 1 M boron tribromide (BBr_3) in CH_2Cl_2, dimethyl sulfoxide (DMSO; anhydrous, 99%), *N,N*-dimethylacetamide (DMAc; anhydrous, 99%), and triethylamine were obtained from Aldrich Chemical Co. and were used without further purification. Methacryloyl chloride (tech., 90%) was distilled before use. Azobis(isobutyronitrile) (AIBN; Alfa) was recrystallized from methanol prior to use.

Characterization. Melting points (T_m) of the monomers and glass transition temperatures (T_g) of the polymers were measured using a Perkin-Elmer DSC-7 differential scanning calorimeter under nitrogen (50 mL/min). Samples were cooled rapidly after each scan using a Perkin-Elmer refrigerator unit (Model No. FC-60-PEA). The onset of the change in slope to the minimum of the endotherm peak was recorded as the T_m value (heating rate = 10 °C/min), while T_g values were taken from the midpoint of the change in slope of the baseline (heating rate = 10 °C). Weight loss data were obtained using a Perkin-Elmer TGA-7 thermogravimetric analyzer at a heating rate of 10 °C/min in air (50 mL/min). Inherent viscosity values were obtained in DMAc (26.5 °C; 0.5 g/dL) with a calibrated Ubbelohde viscometer. A Haake D8 immersion water heater was employed to control the bath temperature. ^{1}H-NMR were recorded on a Bruker AM 360 spectrometer at 360.1 MHz in $CDCl_3$ or DMSO-d_6 and referenced to $Si(CH_3)_4$. Analytical thin layer chromatography (TLC) was run using commercial Kieselgel plates coated with silica gel F-254 (0.25 mm thick). Elemental analyses were obtained from Robertson Microlit Laboratories, Madison, NJ. Electrochemical measurements were made with a PAR Model 173 potentiostat and a Model 175 voltage programmer and were recorded on a Asea Brown Boveri X-Y recorder. Cyclic voltammograms were measured in argon-flushed spectrochemical grade (Burdick and Jackson) DMF containing 0.1 M tetrabutylammonium hexafluorophosphate (recrystallized from EtOH) . The concentration of electroactive species was approximately 1 mg/mL. The working electrode was a 1 mm diameter platinum disk; the counter electrode was a platinum wire, and the reference electrode was a commercial saturated calomel electrode. Photographs of the PBD/PMMA crystal structures were obtained using a Nikon AFX-DX camera attached to a Nikon OPTIPHOT2-POL microscope equiped with a Mettler FP82 hot stage controlled by a Mettler FP80 central processor.

(39) Unfortunately the deposition solvent in ref 35 was not disclosed.

Synthesis. Poly(2-phenyl-5-(3′-((methacryloyl)oxy)phenyl)-1,3,4-oxadiazole) (2a). Typical procedure: THF (Aldrich anydrous grade) was passed through a plug of basic alumina, and 9.0 mL was used to dissolve 1.00 g (3.29 mmol) of monomer AIBN (8.5 mg, 52 mmol) was added and the resulting solution degassed with a stream of Ar. The polymerization was carried out for 21.5 h at 53 °C under Ar. The reaction mixture was diluted to 20 mL, and precipitated into 200 mL of MeOH, and collected by filtration. The crude polymer was redissolved in THF, filtered through Celite, and precipitated into MeOH. Filtration and drying yielded 0.726 g (73%) of a white solid. Anal. Calcd for $C_{18}H_{14}O_3N_2$: C, 70.58; H, 4.61; N, 9.15; O, 15.67. Found: C, 69.84; H, 4.59; N, 8.91; O, 16.29.

Poly(2-phenyl-5-(4′-(methacrylamido)phenyl)-1,3-oxazole) (2b). Typical procedure: THF (Aldrich anydrous grade) was passed through a plug of basic alumina, and 2.5 mL was used to dissolve 0.506 g (1.66 mmol) of monomer. AIBN (3.5 mg, 21 mmol) was added and the resulting solution degassed with a stream of Ar. The polymerization was carried out at 55 °C for 57 h under Ar. The reaction mixture was precipitated into 50 mL of MeOH, yielding 0.267 g of polymer. The crude polymer was redissolved in THF, passed through a 0.45 μm syringe filter, and precipitated into MeOH. Filtration and drying yielded an off-white solid. Anal. Calcd for $C_{19}H_{16}N_2O_2$: C, 74.98; H, 5.30; N, 9.21; O, 10.51. Found: C, 72.62; H, 5.45; N, 8.84; O, 12.77.

Poly(formal)s 7 and 11. These polymers were synthesized according to literature procedure[26] and were run at high concentration to limit the amount of cyclics. Typical procedure: To a 15 mL round-bottomed flask containing 1.0 g (2.52 mmol) biphenol **1b** was added 2 mL of NMP and 1.33 mL of CH_2Cl_2. The solution was stirred for 5 min. A 0.50 g (8.9 mmol) sample of 85% KOH pellets and 0.012 g (0.025 mmol) of 3,5-di-*tert*-butylphenol were added all at once, and the solution was heated to 70 °C. After 4.5 h the viscous solution was diluted with ca. 4 mL of DMAc and added dropwise to 200 mL of isopropanyl alcohol: H_2O:AcOH (80:80:40 mL) being stirred rapidly in a Waring blender. The white fibrous polymer was collected by filtration, washed (isopropyl alcohol, H_2O, and isopropyl alcohol), and dried.

Poly(aryl ether)s 8–10 and 12–14. Typical procedure: To a 50 mL three-neck round-bottomed flask equipped with a Dean–Stark trap, cold water condenser, thermometer, and nitrogen inlet were added 0.8 g (3.147 mmol) of 2,5-bis(3′-hydroxyphenyl)oxadiazole **1a**, 0.8 g (3.147 mmol) of 4,4′-difluorodiphenyl sulfone, 0.522 g (3.78 mmol) of anhydrous potassium carbonate, ca. 6 mL of toluene, and 8 mL of DMSO. The mixture was heated to reflux, and toluene was removed incrementally to provide the following reaction temperatures: 137 °C (0.5 h), 142–145 °C (4 h). The mixture was diluted with ca. 6 mL of DMAc, filtered, added dropwise to isopropyl alcohol: H_2O:AcOH (150:150:75 mL), and stirred rapidly in a Waring blender. Filtration of the precipitate, washing (isopropyl, H_2O, and isopropyl alcohol) and drying gave 1.34 g (90% yield) of a white fibrous precipitate. The polymer was redissolved in 30 mL of $CHCl_3$, filtered through a thin bed of silica gel, precipitated, and isolated as described.

Device Preparation. Typical device configuration on glass: ITO (Balzer's Low Ohmic ITO glass; Fremont, CA), PPV (1100 Å), electron transporter (450 Å; polymer or small molecule), and aluminum (1500–2000 Å). All devices were prepared under an inert atmosphere in a glovebox. Each device (1 × 1 cm) was composed of 121 circular diodes. Typical method of preparation: ITO coated glass substrates were cleaned in an ultrasound bath with solvents as follows: methanol, acetone, 1,1,1-trichloroethane, isopropyl alcohol, acetone, and methanol. The tetrahydrothiophenium precursor salt of PPV, prepared as described previously,[40,41] was dissolved in methanol and deposited onto ITO coated glass by spin-coating (2000 rpm for 120 s; 1/4 acceleration). The precusor polymer thickness was ca. 850 Å before curing. Thermal conversion to PPV was done in a forming gas atmosphere (15% H_2 and 85% N_2) using the following temperature ramp: 25 °C (1 h), 25 to 200 °C (4 h), 200 °C (4 h). A second layer of the precusor polymer was then spin-coated and cured as follows: 25 °C (1 h), 25 to 200 °C (5 h), 200 °C (6 h). Total thickness of the PPV double layer = 1100

(40) Papadimitrakouplos, F.; Konstadinidis, K.; Miller, T. M.; Opila, R.; Chandross; E. A.; Galvin, M. *Chem. Mater.* **1994**, *6*, 1563.

(41) All of the devices were prepared from the same batch of the precursor salt.

Å. The PPV single-layer devices were prepared as described[40] and were also 1100 Å. The ET polymer layer was deposited by spin coating (2000 rpm for 1 min; full acceleration) from dilute solution (2% w/v). The solvents used were: poly(aryl methacrylate)s **15** and **16** (chlorobenzene), poly(formal) **11** and poly(aryl ether) **9** (dimethylacetamide), and poly(aryl ether)s **8** and **10** and **12**–**14** (cyclohexanone). The thickness of the ET layer as measured by Dectak was in the range 450–500 Å. The aluminum electrode (2000 Å) was deposited by thermal evaporation through a shadow mask from a tungsten filament at $<10^{-6}$ Torr. All evaporations were done at 4–7 Å/s at 1.2×10^{-6} torr.

The xanthate precursor polymer was prepared as previously described.[31] Thin films were deposited by spin coating (2000 rpm for 1 min) from cyclohexane (ca. 25 mg/mL). Thermal conversion was carried out under Ar using the following temperature ramp: 25–180 °C (4 h) and 180 °C (6 h). Film thickness after curing was 1000 Å.

Electroluminescence Measurements. The LEDs were 1 mm^2 in area and were driven with direct currents up to 5 A/cm^2 which required bias of 10–60 V. Device characteristics were measured in air using a two-probe (Wentworth Labs; Model No. PR-240) technique. External quantum efficiencies were measured by placing each device directly on top of a calibrated silicon photodiode whose response was measured by a Hewlett Packard 4155A semiconductor parameter analyzer . Internal quantum efficiencies were subsequently calculated from these values using the assumptions put forth by the Cambridge group.[42] Specifically, the external values were multiplied by $2n^2$, where n is the refractive index of glass. To be conservative a value of 1.5 was used for n. Devices were stored in an Ar- filled drybox between measurements.

Acknowledgment. M.S. was partially supported by a NSERC/NATO postdoctoral fellowship (1992–1994). We thank Mr. Fred C. Schilling for the molecular simulations and Drs. Mohan Srinivasarao and Karl R. Amundson for help with the photomicrographs. Useful comments on the manuscript by Dr. Edwin A. Chandross and Dr. Lewis J. Rothberg are appreciated.

Supporting Information Available: Text giving experimental details and figures showing structures, minimum energy conformations, a DSC scan, photomicographs, and a current/voltage plot (19 pages). This material is contained in many libraries on microfiche, immediately follows this article in the microfilm version of the journal, can be ordered from the ACS, and can be downloaded from the Internet; see any current masthead page for ordering information and Internet access instructions.

JA951725J

(42) Greenham, N. C.; et al. *Adv. Mater.* **1994**, *6*, 491.